Ege Coğrafya Dergisi, 25/2 (2016), 1-14, İzmir
Aegean Geographical Journal, 25/2 (2016), 1-14, Izmir—TURKEY

DETECTING TRENDS IN FOREST DISTURBANCE AND RECOVERY USING LANDSAT IMAGERY IN TURKEY

Türkiye'de Orman Bozunumu ve Geri Kazanımı Eğiliminin Landsat Görüntüler ile Belirlenmesi

Doğukan Doğu YAVAŞLI

Ahi Evran Üniversitesi Fen – Edebiyat Fakültesi Coğrafya Bölümü Kırşehir
dogukan.yavasli@ahievran.edu.tr

Shannon FRANKS

SGT, Inc., NASA Goddard Space Flight Center, Greenbelt, Maryland, USA
shannon.franks@nasa.gov

Abstract

Forest disturbance and recovery plays an important role for forest ecosystem management. Understanding the temporal and spatial pattern of these processes is crucial as they affect the carbon flux between atmosphere and biosphere. In this study, the disturbance and recovery processes of forests in Turkey between the years 2000-2010 were detected by Landsat imagery using the LEDAPS Disturbance Index (DI) algorithm. We used validation data collected by field works and achieved 90% overall accuracy with 32 observation points for our resulting map. The comparison with various high resolution data also demonstrated that the DI algorithm can be effectively used to detect forest disturbance and recovery processes in Turkey.

Keywords: Forest disturbance, Forest recovery, Landsat

Öz

Orman bozunumu ve geri kazanımı orman ekosisteminin yönetiminde önemli rol oynar. Biyosfer ve atmosfer arasındaki karbon değişimini etkilemesi bakımından bu süreçlerin zamansal ve mekânsal dokusunu anlamak kritiktir. Bu çalışmada 2000 – 2010 yılları arasında Türkiye'deki ormanların bozunum ve geri kazanım süreçleri Landsat görüntüler ve LEDAPS Disturbance Index (DI) algoritması kullanılarak belirlenmiştir. Arazi çalışmaları sonucunda 32 adet gözlem noktasından toplanan doğrulama verileri ile %90 oranında doğruluk elde edilmiştir. Çeşitli yüksek çözünürlüklü uydu görüntüleri de DI algoritmasının Türkiye'de orman bozunum ve geri kazanım süreçlerinin belirlenmesinde kullanılabileceğini göstermiştir.

Anahtar Kelimeler: Orman bozunumu, Orman geri kazanımı, Landsat

1. Introduction

Forest disturbance and recovery play an important role in regional and global carbon budgets. The carbon balance of a forest ecosystem is primarily based on its disturbance and recovery processes. Forest disturbance can be defined as a relatively discrete event causing a change in the physical structure of the vegetation and the surface soil (Clark, 1990). On the other hand, forest recovery refers to the reestablishment or redevelopment of forest biomass and canopy structure characteristics after the impact of a disturbance. It should be noted that although these definitions include disturbances or recoveries from falling or regeneration of branches, to landscape level changes, the disturbance and recovery terms used in this study refers to the ones that are detectable by satellite based imagery.

While forest disturbances may cause immediate release of carbon with fires or may transfer biomass from living vegetation to dead material that decomposes over a period of years; forest recoveries tend to sequester carbon from the atmosphere with an increasing trend over years as the recovery process starts (Chambers et al., 2004). The balance of these processes plays an important role in the net terrestrial sink in concern with global carbon budgets.

Uncertainties and the change over time and space is also crucial to understanding these processes. In recent years, there have been many studies and advanced algorithms on assessing spatial and temporal pattern of forest disturbance. For instance, Masek et al. (2008) developed a disturbance mapping algorithm and assessed the forest disturbance of North America from the early 1990's to 2000's. Likewise, Huang et al. (2009) used time series stacks of Landsat images to evaluate the dynamics of seven national forests in eastern United States. Huang et al. (2009) used a Vegetation Change Tracker (VCT) algorithm to map the year of forest disturbance and had accuracies for forest disturbance about 80%. But users and producer's accuracies for many disturbance classes were considerably lower. Hais et al. (2009) assessed Landsat images from 1985 to 2007 to detect disturbance at Šumava Mountains (Czech Republic) using spectral indexes such as Normalized Difference Vegetation Index (NDVI), Tasseled Cap Transformation, Disturbance Index (DI) and DI'. They found that DI' shows the highest sensitivity to forest disturbance for different disturbance types like clear-cuts and bark beetle outbreak. Kennedy et al. (2010) developed an algorithm called Landsat based detection of trends in disturbance and recovery (LandTrendr) to extract spectral trajectories of land surface change from Landsat images. They tested their algorithm over Pacific Northwest, USA and claim that it may be feasible for various ecoregions. Similarly, Zhu et al. (2012) developed a new change detection algorithm called Continuous Monitoring of Forest Disturbance Algorithm (CMFDA) for continuous monitoring of forest disturbance. They indicate that their algorithm is higher than 95% accurate for detecting forest disturbance.

In this study we assessed the disturbance and recovery of Turkey's forests through the Disturbance Index (DI) algorithm that was formerly produced by Masek et al. (2008). The DI algorithm was a part of The Landsat Ecosystem Disturbance Adaptive Processing System (LEDAPS) project, which has been funded by NASA to develop a robust system for processing large quantities of Landsat data for forest change analysis. Although the North American disturbance and recovery data products are already developed through the LEDAPS project, in this study we tried to assess the forest disturbance and recovery of another area, Turkey. As well as the main purpose of this study being to quantify and map the disturbance and recovery; two other outcomes were also projected: 1) to evaluate the LEDAPS algorithm in a different area with differing physical geography conditions and 2) to update Turkish Ministry of Forest and Water measurements of forest cover as they are likely outdated.

2. Study Area

Turkey is located in the northern hemisphere between 36–42° N and 26–45° E and is surrounded by four seas: the Mediterranean to the south, the Aegean to the west, the Sea of Marmara between the continents of Europe and Asia, and the Black Sea to the north. In Turkey, forests cover 27.2% of the 80 million hectares of national territory. Almost half of these forested areas have less than 10% canopy cover and are considered as degraded forest by the Turkish Ministry of Forest and Water

General Directorate of Forestry (GDF) (OGM, 2006). The government owns more than 99.5% of forest resources and management is implemented by the GDF; with the remainder owned by public or private entities. High forest accounts for 73% of total forest, and coppice forest for 27%. High forest covers three types of forest stand: coniferous, broadleaf and mixed with 74, 12 and 14% respectively (Guneş and Coşkun, 2008). Main species that exists in order of the coverage area are Oak (*Quercus sp.*), Calabrian Pine (*Pinus brutia Ten.*), Crimean Pine (*Pinus nigra Arnold*) and Beech (*Fagus sp. L.*). 60 % of the country's forest areas are dominated by coniferous species, especially Calabrian Pine and Crimean Pine while the broadleaved species, particularly oaks dominate 40 %. (OGM, 2009). Precipitation rates vary greatly in Turkey and are a major factor on the distribution of the forest, with most of the forested areas being along the coastal regions, where precipitation rates are higher.

3. Data Set and Preprocessing

The Global Land Survey (GLS) data sets are cloud-free, orthorectified collections of Landsat imagery that are designed to support global land-cover and ecological monitoring (Gutman et al, 2008). In this study we used the GLS 2000 and 2010 data sets of Turkey, augmented with other Landsat 5 and Landsat 7 imagery when needed. The selection of imagery was highly important. In most cases, the GLS dataset imagery was optimal because it maximized summer seasonality through the NDVI metric (Franks et al., 2009). We tried to ensure all imagery had similar time period to represent similar phenological stages of the year. In geographic areas where GLS 2000 and 2010 data was not resembling, we selected and processed other Landsat 5 or Landsat 7 imagery.

All the imagery was calibrated and atmospherically corrected to surface reflectance by Earth Resources Observation and Science (EROS) data center using the MODIS 6S radiative transfer approach defined in Masek et al. (2006). Additionally, all GLS data were terrain corrected and registered to the 2000 dataset, so to provide a consistent geographic base.

In addition to the above-mentioned data, we also used some supportive data to validate our study and to test the algorithm. One of these is the CORINE (Coordination of information on the environment) (EEA, 2007) dataset of land cover for 2000 and 2006. CORINE dataset is a land cover distribution map and is produced for European countries. Also we obtained 1/25.000 scale stand maps from GDF that were recently updated in 2011. Even though these maps cover only a part of the area in southwest Turkey, that region was where we did field work for validation so it was very useful as a reference. We also used some unclassified high-resolution data obtained from NGA through a partnership with the Civil Applications Committee (CAC), of which NASA is a member (Neigh et al., 2013).

4. Disturbance Index (DI) Algorithm

The DI algorithm we used in the study is a linear combination of the three Tasseled-Cap indices: Brightness, Greenness and Wetness (Crist and Cicone, 1984; Kauth and Thomas, 1976). The Tasseled Cap transformation reduces the Landsat reflectance bands to these three orthogonal indices and is commonly used in disturbance mapping studies due to its ability to detect vegetation changes. The DI algorithm is based on the hypothesis that recently cleared forestland exhibits high Brightness and low Greenness and Wetness in relation to undisturbed forest (Healey et al., 2005). The DI transformation is calculated using the eq. 1:

$$DI = B' - (G' + W') \tag{1}$$

where B', G', and W' represent the Tasseled-Cap brightness, greenness, and wetness indices normalized by a dense forest class for each Landsat scene, such that (for example):

$$B' = (B - \mu B)/\sigma B \tag{2}$$

where μB is the mean Tasseled-Cap brightness index of the dense forest class for a particular scene, and σB is the standard deviation of brightness within the dense forest class for a particular scene. The resulting DI image is a single band image with the values greater than a certain threshold having a high probability of being disturbed or non-forest and values closer to zero being likely dense forest or undisturbed.

The steps to create disturbance index are as follows: (Figure 1)

The first step is calculation of Tasseled-Cap. Tasseled-Cap indices were calculated for each selected image from the 2000 and 2010 surface reflectance datasets using the reflectance factor transform of Crist (1985).

After that we normalized Tasseled-Cap as step 2. For normalization of Tasseled-Cap images, we needed to identify a “dense forest” class for each GLS image. We used the MODIS Vegetation Continuous Fields (VCF) product (Hansen et al., 2002) and a normalized difference vegetation index (NDVI) image for dense forest classes. A threshold was chosen to identify reflectance values to represent forest pixels for both parameters (see Table 1). TM/ ETM+ pixels having higher values than VCF_thresh and NDVI_thresh for VCF cover and NDVI respectively were identified as likely “pure” forest pixels. It should be noted that the normalization step occurred independently for each scene and tended to suppress the effects of scene-to-scene variability in overall reflectance due to small changes in bi-directional reflectance distribution function or phenology. In most cases the same thresholds were used for all imagery, but in cases where the image phenology was significantly different, a new set of thresholds were used to ensure that there was a sufficient amount of training pixels (ie. dense forest pixels) available.

Third step is the DI and ΔDI calculation. Given the population of mature forest pixels from step 2, the mean and standard deviation of each Tasseled-Cap component for the class were calculated. The normalization of each Tasseled-Cap image plane executed as in equations (1) and (2). The ΔDI was calculated as the temporal change of DI2010–DI2000 where large positive values of ΔDI corresponded to likely disturbance events; large negative values corresponded to likely recovery. We defined thresholds to the ΔDI values to identify such disturbance and recovery.

Step 4 is filtering non-forest change. Other land-cover transformations such as agricultural patterns may be inadvertently identified by these ΔDI trends. Removing these artifacts was performed by screening the map with a forest/non-forest mask that was produced independently for each image (2000 and 2010). We used a “fuzzy classifier” that blended three metrics indicative of forest cover: (1) the MODIS VCF tree cover product; (2) the DI value itself; and (3) the ratio of red reflectance (ρ3) to NDVI (redNDVI). These metrics were transformed to independent estimates of probability of membership in the forest class (P) according to:

$$P_{VCF} = \{0 \text{ for } VCF < \%20,\ VCF/VCF_{max} \text{ for } VCF\} \quad (3)$$

$$P_{DI} = e * [-(\alpha DI)^2/2] \quad (4)$$

$$P_{redNDVI} = 1/ [1+e^{v*(\rho3/NDVI+ \eta)}] \quad (5)$$

where VCFmax represents the local upper bound on tree cover as recorded by the MODIS VCF product, and α, v, and η are empirical scaling parameters used to scale the raw metrics (DI, redNDVI) for the Gaussian probability function (4) or sigmoid probability function (5). The overall probability of forest class membership (P_f) was calculated as a weighted sum of the three independent metrics:

$$P_f = W_{VCF}P_{VCF} + W_{DI}P_{DI} + W_{redNDVI}P_{redNDVI} \quad (6)$$

where the sum of the weighting factors (w) are constrained to unity. A high value of P_f (>~0.6) indicates that the pixel is likely to be forested.

The classifier was not particularly sensitive to the exact threshold in P_f, since the vast majority of pixels tended to cluster at either very low or very high values of P_f. If either or both the circa-2000 and/or circa-2010 pixel was labeled as ‘forest’, then the pixel is retained in the disturbance/recovery map. Table 2 gives sample parameter values for the forest/non-forest classification for Turkey.

Last step is Post-processing. Three final sub-steps were implemented to finalize the disturbance map. First, a 5×5 pixel sieve filter is used to remove small patches of disturbance or recovery, including “speckle” associated with slight misregistration in the imagery. This filter also imposed a ~0.50 ha minimum-mapping area on the products since the GLS pixel resolution is 30 m. After that a water mask that is based on near-infrared reflectance was calculated for each scene, and any water pixels were removed from the map. Finally, to screen out agricultural pixels that were not correctly filtered in step 4, we used the CORINE dataset to mask out any remaining pixels.

This insured that any variations that the delta DI algorithm classified as disturbance or recovery were of forest and not a product of agriculture shifting.

5. Algorithm Validation Calibration and Fieldwork

Masek et al. (2008) noted that the DI algorithm requires multiple parameters that can be "tuned" for a particular geographic area. In this study we used the validation data as "training" to constrain and optimize the parameter selection. Before the disturbance and recovery map was calculated using the DI statistics, it was important that the forest map classification was correct because this was used to screen out (i.e. mask) the non-forest dynamics.

Examining our selected training area, Muğla province at the southwest coast of Turkey, we noticed that there were some incompatibilities about the forest – non-forest differentiation of the DI algorithm and the stand maps acquired from GDF. We noticed this especially in areas covered with scrubland vegetation of the region called "maquis", which was causing confusion for the DI algorithm. Maquis typically consist of densely growing evergreen shrubs or small trees such as holm oak and spurge olive and are typically 2-4 m in height (Makhzoumi, 1999). Maquis makes it harder to discriminate forests and non-forest areas due to having dense vegetation cover. We noticed that some maquis areas were classified as forest with our algorithm while the stand maps call the same patch non-forest. A similar problem was found in areas called "degraded forest" by stand maps. Many of these areas are "forest" as a land use and classified as degraded forest even though there is no forest cover at all. For our purposes, we were not necessarily concerned whether the land use was classified as "forest" or not, although we will often refer to it as such, but whether there was biomass present or not. Regardless, the difference in what our algorithm was reporting and what the Turkish ministry reported caused indecision as to what the vegetation was actually like there.

To overcome these issues and to have ground truth data, we carried out a field campaign to some of these areas in late August 2012. Fifty-five (55) locations were visited (Figure 2) and the land cover types were examined while collecting approximate vegetation height and canopy closure. The fieldwork was constrained to areas that were nearby roads since much of this area is not easily accessible. The points that were collected were representative of a larger area to minimize edge effects. Photos were taken as well as data collected. The basic attribute that we were trying to determine was whether biomass was present. This was determined if the vegetation had woody stems. Forested lands were recorded as positive for biomass as were maquis, if woody stems were present. This confirms what most literature also reported (De Jong et al., 2003; Sağlam et al., 2008; Tolunay, 2011). It was this knowledge that was used to validate the Landsat forest classification map.

Additionally, our individual interviews with forest engineers from Muğla District Office of Forestry supported our approach. We have been told that the stand maps, which were derived in 1990's, do not classify maquis as forested areas due to a few reasons. First, the foresters cannot use the maquis economically to produce firewood. Second, some maquis do not have 10% canopy cover and/or enough tree height to be classified as forest since they are degraded pine or oak forests. However, because of the recent studies that show high biomass densities of maquis, the foresters decided to classify these areas as forest in future stand map updating studies.

Since the Landsat forest classification map solely recorded whether an area was forested or not and we compared those results to our field work to determine if that was true, a comprehensive contingency map with producer's and user's accuracy was not feasible. Instead, the overall accuracy of our Landsat derived forest map was calculated for 32 observations and was over 90% (29 correct). There were 23 places that we observed from a distance but we were not able to collect data on so they were not included in the accuracy analysis but rather used for general knowledge of the area. It was interesting that in each case (there were only 3) where the Landsat forest map and our fieldwork disagreed it was an error of omission (pixels mistakenly mapped as non-forest) on the part of the Landsat derived forest map.

Visual interpretation is also one of the most reliable approaches for analyzing satellite imagery because of the ability of human eyes to combine spectral, spatial (including texture and contextual information), and temporal information in image analysis (Huang et al., 2009). Figure 3 shows disturbance/recovery examples derived from Landsat and other commercial high resolution satellite images acquired before and after the occurrence of them.

6. Results and Conclusions

We mapped forest disturbance and recovery across Turkey during the 2000-2010 interval together with a forest/nonforest map (Figure 4). Results indicate that in 10 years 238,762 ha forest was disturbed while 322,583 ha forest regrew making a contribution of %1 rise in forest areas in Turkey (Table 3).

The distribution of forest disturbance and recovery in Turkey can be observed better in provincial basis (Figure 5).

The statistics and fire records obtained from GDF shows that fires cause half of the disturbance whereas afforestation areas are much higher than recovery areas detected by the algorithm (Table 4). This issue is related with the occurrence of both events. Disturbances arises from fires are sudden events and can be detected easily with ten-year interval satellite imagery. However, recovery due to afforestation will result as a forest cover in a delayed way.

On the other hand, the pattern of the disturbance and recovery is found to be different. While the disturbance occurs in larger patches, recovery areas appear in smaller patches. We think this shows that the disturbance regime is mostly due to anthropogenic activities such as fire or logging whereas recovery is mostly caused by natural activities.

There can be noticed a forest areal extent difference between the GDF stats and our calculations. Most of the difference is derived from the definition of forests as we also mention above (section 5). Subtracting the degraded forests from total forest area, our calculations are very close with productive forest areas obtained from GDF. Another source of difference is the cloud cover. Even though we choose cloud free or less cloudy images for all periods, there are some parts, especially the northern shores of Turkey, which has more clouds and shadow.

Not surprisingly, the algorithm has not performed equally well for all scenes/parts of Turkey. Images that were acquired at widely separated parts of the seasonal growing cycle tend to exhibit high error rates. The ΔDI approach is self-normalizing, in that the Tasseled- Cap norming population comes from each image independently, and thus tends to resist small changes in bi-directional reflectance distribution function and image phenology. However, when these changes become extreme (e.g. leaf-on vs. leaf-off seasonality), the ΔDI method breaks down. A good example of this situation is seasonally changeable areas like croplands and grasslands, which can be confused with forests if the image selection date of the year is not similar. In this case these areas can be classified as forest and the change in the second imagery may result as disturbance or recovery. Our cropland mask derived from CORINE dataset mostly solved this problem in croplands but grasslands can remain if the imagery selection is not very well.

Finally, we acknowledge that 10 year repeat interval is not ideal for accurately mapping forest disturbance and recovery. However, this study demonstrates automated approach for mapping disturbance and recovery process and first wall-to-wall country scale disturbance/recovery map of Turkey.

REFERENCES

Chambers, J. Q., N. Higuchi, L. M. Teixeira, J. D. Santos, S. G. Laurance, S. E. Trumbore. 2004. "Response of tree biomass and wood litter to disturbance in a Central Amazon forest" *Oecologia*, **141**: 596 – 614.

Clark, D. B. 1990. "The role of disturbance in the regeneration of neotropical moist forests, in Reproductive Ecology of Tropical Forest Plants" *Man in the Biosphere Series*, **Vol. 7**, edited by K. S. Bawa and M. Hadley, pp. 291–315, U. N. Educ., Sci., and Cult. Org., Paris.

Cohen, W. B., Spies, T. A., Fiorella, M. 1995. Estimating the age and structure of forests in a multi-ownership landscape of western Oregon, U.S.A., *International Journal of Remote Sensing*, **16**: 721-746.

Crist, E. P., Cicone, R. C. 1984. "Application of the Tasseled-Cap concept to simulated Thematic Mapper data" *Photogrammetric Engineering and Remote Sensing*, **50**: 343−352.

Crist, E. P. 1985. "A TM tasseled cap equivalent transformation for reflectance factor data" *Remote Sensing of Environment*, **17**: 301−306.

De Jong, Steven M., Edzer J. Pebesma, Bernard Lacaze. 2003. "Above-ground biomass assessment of Mediterranean forests using airborne imaging spectrometry: the DAIS Peyne experiment" *International Journal of Remote Sensing* **24** (7): 1505-1520.

European Environment Agency (EEA). 2007. *CLC2006 technical guidelines*, No: 17. Retrieved from http://www.eea.europa.eu/publications/technical_report_2007_17 on April 2012.

FAO, 2001 *Global Forest Resources Assessment 2000 Main Report* . FAO Forestry Paper 140 .

Franks, S., J. Masek, R. Headley, J. Gasch, T. Arvidson. 2009. "Large Area Scene Selection Interface (LASSI). Methodology of Selecting Landsat Imagery for the Global Land Survey 2005" *Photogrammetric Engineering & Remote Sensing*, **75** (11): 1287-1296

Frolking, S., M. W. Palace, D. B. Clark, J. Q. Chambers, H. H. Shugart, G. C. Hurtt. 2009. "Forest disturbance and recovery: A general review in the context of spaceborne remote sensing of impacts on aboveground biomass and canopy structure" *Journal of Geophysical Research* **114** (July 22).

Güneş, Y., Coşkun, A. A. 2008. *Trends in forest ownership, forest resources tenure and institutional arrangements: are they contributing to better forest management and poverty reduction? A case study from Turkey*. Food and Agricultural Organization of the United Nations, Rome, Italy.

Gutman, G., R. Byrnes, J. Masek, S. Covington, S, C. Justice, S. Franks, R. Headley, 2008. "Towards monitoring land cover and land-use changes at a global scale: The Global Land Survey 2005", *Photogrammetric Engineering & Remote Sensing*, **74** (1):6-10

Hais, Martin, Magda Jonášová, Jakub Langhammer, Tomáš Kučera. 2009. "Comparison of two types of forest disturbance using multitemporal Landsat TM/ETM+ imagery and field vegetation data" *Remote Sensing of Environment* **113** (4) (April): 835-845. doi:10.1016/j.rse.2008.12.012.

Hansen, M.C., Potapov, P.V., Moore, R., Hancher, M., Turubanova, S.A., Tyukavina, A., Thau, D., Stehman, S.V., Goetz, S.J., Loveland, T.R., Kommareddy, A., Egorov, A., Chini, L., Justice, C.O., Townshend, J.R.G. 2013. "High-resolution global maps of 21st century forest cover change" *Science*, **342** (6160): 850-853.

Healey, S, W. Cohen, Y. Zhiqiang, O. Krankina. 2005. "Comparison of Tasseled Cap-based Landsat Data Structures for Use in Forest Disturbance Detection." *Remote Sensing of Environment* **97** (3) (August 15): 301–310. doi:10.1016/j.rse.2005.05.009.

Huang C, Goward S N, Schleeweis K, Thomas N, Masek J G, Zhu Z. 2009. “Dynamics of national forests assessed using the Landsat record: Case studies in eastern United States.” *Remote Sensing of Environment* **113** (7): 1430-1442.

Huang, C., Wylie, B., Yang, L., Homer, C., & Zylstra, G. 2002. “Derivation of a Tasseled-Cap transformation based on Landsat-7 at-satellite reflectance” *International Journal of Remote Sensing*, **23**, 1741−1748.

Kauth, R. J., Thomas, G. S., 1976. “The tasseled cap --a graphic description of the spectral-temporal development of agricultural crops as seen in Landdat”, in *Proceedings on the Symposium on Machine Processing of Remotely Sensed Data*, West Lafayette, Indiana, June 29 -- July 1, 1976, (West Lafayette, Indiana: LARS, Purdue University), 41-51.

Kennedy, Robert E., Zhiqiang Yang, Warren B. Cohen. 2010. “Detecting trends in forest disturbance and recovery using yearly Landsat time series: 1. LandTrendr — Temporal segmentation algorithms.” *Remote Sensing of Environment* **114** (12) (December 15): 2897-2910. doi:10.1016/j.rse.2010.07.008.

Makhzoumi, J. 1999. *Ecological landscape design and planning: the Mediterranean context*. Taylor & Francis.

Masek, J, C Huang, R Wolfe, W Cohen, F Hall, J Kutler, P Nelson. 2008. “North American forest disturbance mapped from a decadal Landsat record.” *Remote Sensing of Environment* **112** (6) (June 16): 2914-2926.

Masek, J.G., E.F. Vermote, N.E. Saleous, R. Wolfe, F.G. Hall, K.F. Huemmrich, F. Gao, J. Kutler, T.K. Lim. 2006. “A Landsat Surface Reflectance Dataset for North America, 1990–2000.” *IEEE Geoscience and Remote Sensing Letters* **3** (1) (January): 68-72.

Neigh, Christopher S., Jeffrey G. Masek, Jaime E. Nickeson (2013). “High-Resolution Satellite Data Open for Government Research” *Eos Trans. AGU,* **94** (13): 121–123.

Orman Genel Müdürlüğü (OGM). 2006. *Orman Varlığımız*. Ankara.

Orman Genel Müdürlüğü (OGM). 2009. *Ormanlarımızda Yayılış Gösteren Asli Ağaç Türleri*. Ankara.

Sağlam, B., Küçük, O., Bilgili, E., Durmaz, B. D., Baysal, İ. 2008. “Estimating Fuel Biomass of Some Shrub Species (Maquis) in Turkey” *Turkish Journal of Agriculture and Forestry*, **32**, 349–356.

Tolunay, D. 2011. “Total carbon stocks and carbon accumulation in living tree biomass in forest ecosystems of Turkey” *Turkish Journal of Agriculture and Forestry*, **35**, 265–279. doi:10.3906/tar-0909-369

Zhu, Zhe, Curtis E. Woodcock, Pontus Olofsson. 2012. “Continuous monitoring of forest disturbance using all available Landsat imagery.” *Remote Sensing of Environment* (February). doi:10.1016/j.rse.2011.10.030.

Tables

Table 1: *Sample parameters for the ΔDI disturbance classification, for Turkey*

Parameter	Purpose	Value
NDVI_thresh	Minimum NDVI for obtaining forest population during Tasseled- Cap normalization	0.65
VCF_thresh	Minimum treecover percentage for obtaining forest population during Tasseled-Cap normalization	55%

Table 2: Parameters for fuzzy classification in Turkey

Parameter	Purpose	Value
VCF_{max}	Normalization for P_{VCF}	60%
α	Scaling for P_{DI}	500
v	Scaling for $P_{redNDVI}$	1000
η	Scaling for $P_{redNDVI}$	150
W_{VCF}	Weight for P_{VCF}	0.25
W_{DI}	Weight for P_{DI}	0.5
$W_{redNDVI}$	Weight for $P_{redNDVI}$	0.7

Table 3: Forest area, disturbance and recovery stats by province in Turkey

Province Name	Forest Area (ha)	Disturbance (ha)	Recovery (ha)	Recovery Disturbance Difference	Percent Tree Cover (2000)	Tree Cover 2000 (ha)	Tree Cover 2010 (ha)
Adana	179 623	10 555	7 760	- 2 795	13%	190 178	187 383
Adıyaman	2 713	87	649	563	0%	2 800	3 362
Afyon	71 490	5 073	2 030	- 3 043	5%	76 563	73 520
Ağrı	5 250	147	1 144	998	0%	5 397	6 395
Aksaray	8 894	5 564	9 409	3 845	2%	14 458	18 303
Amasya	115 383	408	2 136	1 727	20%	115 791	117 519
Ankara	154 275	455	7 397	6 942	6%	154 730	161 672
Antalya	398 556	19 914	30 714	10 800	20%	418 469	429 269
Ardahan	29 252	391	8 742	8 350	5%	29 643	37 993
Artvin	320 940	2 258	2 354	96	42%	323 198	323 295
Aydin	96 590	6 527	3 775	- 2 751	13%	103 117	100 366
Balıkesir	415 547	12 093	7 597	- 4 496	29%	427 640	423 144
Bartın	118 074	461	211	- 249	52%	118 535	118 285
Batman	1 464	3 274	188	- 3 086	1%	4 737	1 652
Bayburt	11 221	94	410	317	3%	11 315	11 632
Bilecik	142 363	1 361	1 203	- 157	34%	143 723	143 566
Bingöl	55 065	2 646	9 097	6 450	7%	57 711	64 161
Bitlis	28 284	1 503	1 164	- 339	3%	29 787	29 447
Bolu	466 311	961	3 460	2 498	55%	467 272	469 770
Burdur	57 275	3 227	1 746	- 1 481	9%	60 502	59 021

Bursa	408 740	5 396	3 722	- 1 674	38%	414 136	412 462
Çanakkale	331 429	3 540	24 842	21 302	34%	334 969	356 271
Çankırı	104 723	352	3 455	3 103	14%	105 076	108 178
Çorum	189 051	322	4 287	3 965	15%	189 373	193 338
Denizli	115 828	6 801	6 308	- 492	10%	122 628	122 136
Diyarbakır	8 329	673	879	205	1%	9 002	9 207
Düzce	156 497	381	299	- 81	59%	156 878	156 796
Edirne	41 246	581	12 794	12 213	7%	41 827	54 041
Elazığ	8 150	371	1 236	865	1%	8 521	9 386
Erzincan	39 774	565	1 011	446	3%	40 339	40 785
Erzurum	171 335	2 091	5 166	3 075	7%	173 427	176 502
Eskişehir	124 883	420	1 987	1 567	9%	125 303	126 870
Gaziantep	5 748	36	294	258	1%	5 784	6 042
Giresun	219 592	603	1 275	672	31%	220 195	220 867
Gümüşhane	118 492	456	1 160	704	17%	118 948	119 651
Hakkari	34 030	9 274	1 365	- 7 909	6%	43 304	35 395
Hatay	114 974	1 528	1 089	- 439	21%	116 502	116 063
Iğdır	7 099	356	943	588	2%	7 455	8 043
Isparta	50 948	2 535	2 180	- 355	6%	53 483	53 127
İstanbul	212 513	6 520	7 796	1 276	42%	219 033	220 309
İzmir	215 825	14 929	9 435	- 5 495	19%	230 754	225 259
K.Maraş	80 378	1 778	1 456	- 323	6%	82 157	81 834
Karabük	242 927	930	5 782	4 852	60%	243 856	248 708
Karaman	6 438	793	450	- 343	1%	7 231	6 888
Kars	26 921	133	4 777	4 645	3%	27 054	31 699
Kastamonu	766 547	1 385	2 938	1 552	58%	767 933	769 485
Kayseri	10 512	520	4 916	4 396	1%	11 032	15 428
Kilis	446	12	39	27	0%	458	484
Kırıkkale	3 425	134	114	- 20	1%	3 559	3 539
Kırklareli	197 276	2 663	23 089	20 426	31%	199 940	220 366
Kırşehir	5 250	234	592	358	1%	5 484	5 842
Kocaeli	149 212	3 478	1 127	- 2 351	45%	152 690	150 339
Konya	46 573	5 135	12 262	7 127	1%	51 707	58 834
Kütahya	269 389	6 828	865	- 5 963	24%	276 217	270 253
Malatya	4 010	195	533	338	0%	4 205	4 544
Manisa	156 927	10 096	1 989	- 8 107	13%	167 023	158 916
Mardin	226	1 179	28	- 1 151	0%	1 405	254
Mersin	113 904	8 801	5 497	- 3 304	8%	122 705	119 401
Muğla	369 743	17 696	18 302	607	30%	387 438	388 045
Muş	13 903	368	722	354	2%	14 272	14 626
Nevşehir	286	72	252	179	0%	358	538
Niğde	4 304	1 389	154	- 1 234	1%	5 693	4 458
Ordu	242 684	544	852	308	40%	243 228	243 536
Osmaniye	87 492	1 286	2 009	723	27%	88 778	89 501
Rize	117 008	77	644	568	30%	117 085	117 653
Sakarya	209 066	2 548	2 298	- 250	44%	211 614	211 363
Samsun	359 996	1 846	6 190	4 343	36%	361 842	366 186
Şanlıurfa	352	85	557	472	0%	437	909
Siirt	8 660	9 170	215	- 8 955	3%	17 830	8 875
Sinop	284 102	597	2 088	1 492	49%	284 699	286 190
Şırnak	26 347	12 573	1 097	- 11 476	5%	38 920	27 444
Sivas	83 061	629	1 898	1 269	3%	83 690	84 959
Tekirdağ	73 774	804	6 672	5 868	12%	74 578	80 446

Tokat	273 497	1 404	3 664	2 260	26%	274 901	277 161
Trabzon	154 936	818	2 240	1 422	33%	155 754	157 176
Tunceli	88 380	1 561	3 191	1 630	11%	89 941	91 572
Uşak	38 109	1 333	171	- 1 161	7%	39 442	38 280
Van	12 085	2 387	4 055	1 668	1%	14 472	16 140
Yalova	44 192	845	287	- 559	59%	45 037	44 479
Yozgat	83 072	1 042	5 242	4 199	6%	84 114	88 313
Zonguldak	157 820	666	621	- 45	48%	158 486	158 441
TOTAL	**10 171 007**	**238 762**	**322 583**	**83 822**	**13%**	**10 409 769**	**10 493 590**

Table 4: Forest fires and afforestation activities in Turkey (OGM, 2010)

Years	Forest Fires (ha)	Afforestation (ha)
2000	26 353	24 494
2001	7 394	25 672
2002	8 514	28 647
2003	6 644	36 914
2004	4 876	34 016
2005	2 821	21 439
2006	7 762	25 319
2007	11 664	18 228
2008	29 749	39 467
2009	4 679	45 422
2010	3 317	41 857
TOTAL	**113 773**	**341 475**

Figures

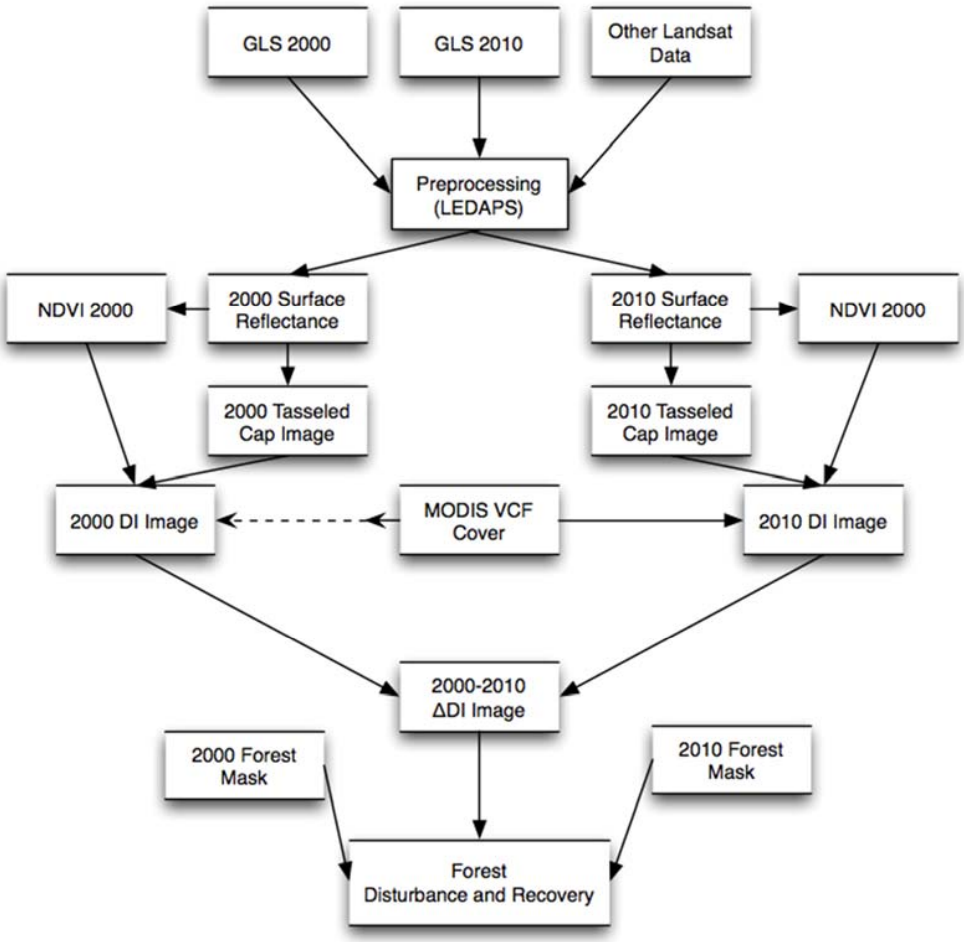

Figure 1: Flow chart of the disturbance/recovery mapping

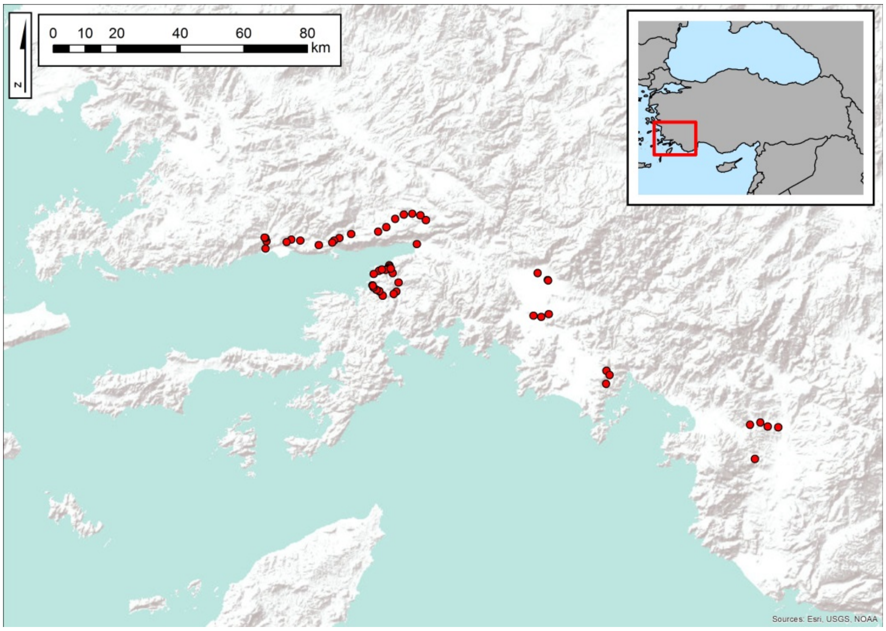

Figure 2: The locations of fieldwork

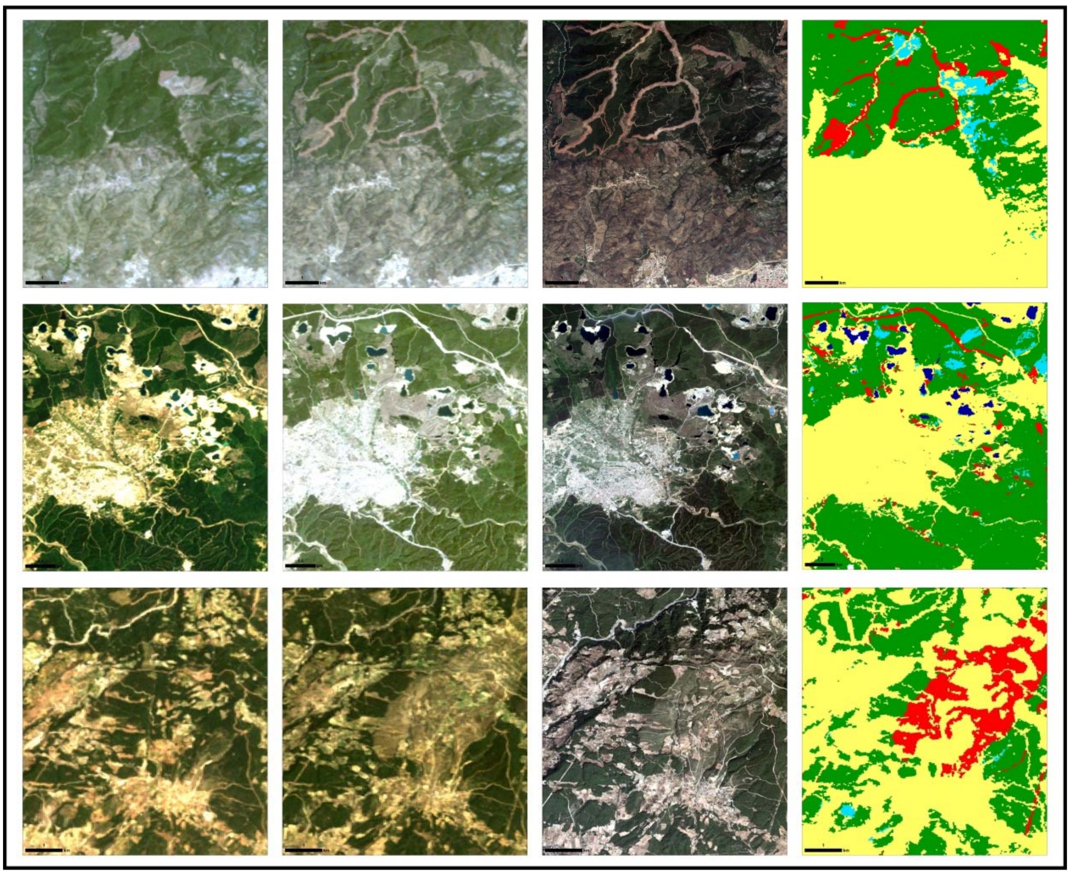

Figure 3: Samples of disturbed and recovered areas. Starting from the leftmost column respectively; 2000 and 2010 Landsat imagery (3-2-1 band combination as RGB), high-resolution satellite imagery of post disturbance/recovery event and the map produced by the algorithm (Figure 4 can be used for the map legend).

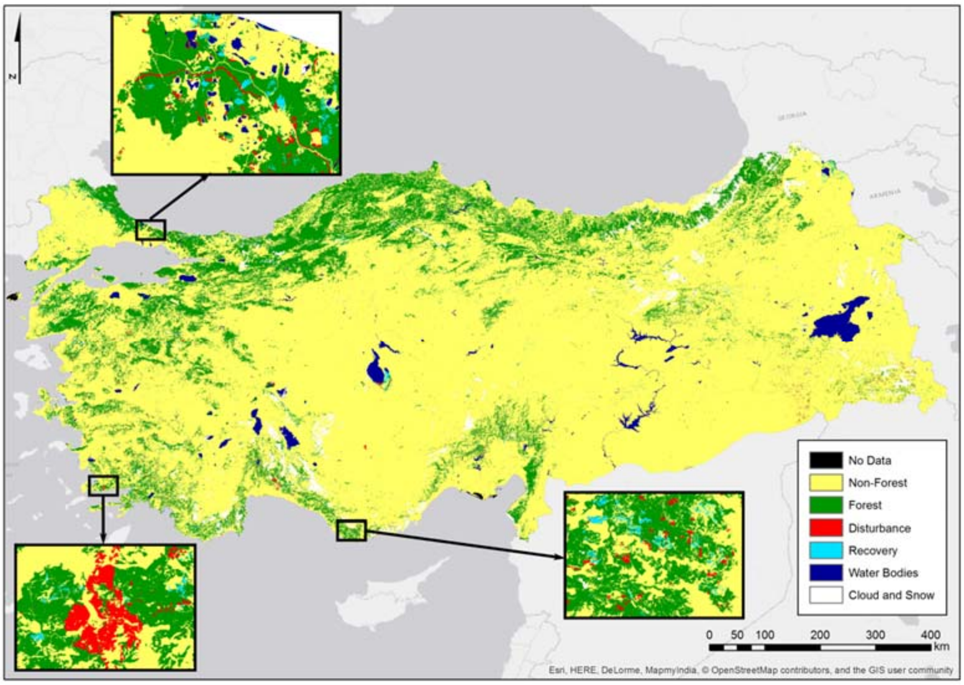

Figure 4: Map of Turkey and selected areas representing disturbance and recovery events from İstanbul, Muğla and Mersin.

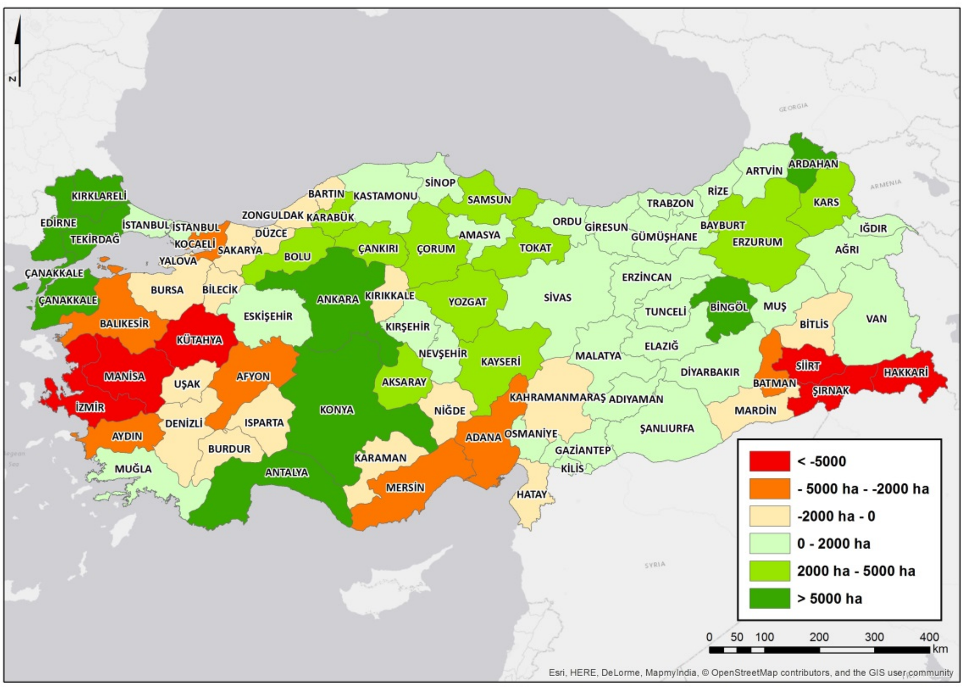

Figure 5: The distribution of net forest disturbance and recovery by province in Turkey between 2000-2010. Negative values represent more disturbance than recovery while positive values represent more recovery than disturbance.